ORIGINAL ARTICLE

Imaging characteristics of supratentorial ependymomas: Study on a large single institutional cohort with histopathological correlation

Sandhya Mangalore, Saritha Aryan[1], Chandrajit Prasad, Vani Santosh[2]

Departments of Neuroimaging and Interventional Radiology, [1]Neurosurgery and [2]Neuropathology, National Institute of Mental Health and Neuroscience, Bengaluru, Karnataka, India

ABSTRACT

Background: Supratentorial ependymoma (STE) is a tumor whose unique clinical and imaging characteristics have not been studied. Histopathologically, they resemble ependymoma elsewhere. We retrospectively reviewed the imaging findings with clinicopathological correlation in a large number of patients with STE to identify these characteristics.

Materials and Methods: Computed tomography (CT) magnetic resonance images (MRI), pathology reports, and clinical information from 41 patients with pathology-confirmed STE from a single institution were retrospectively reviewed. CT and MRI findings including location, size, signal intensity, hemorrhage, and enhancement pattern were tabulated and described separately in intraventricular and intraparenchymal forms.

Results: STE was more common in pediatric age group and intraparenchymal was more common than intraventricular form. The most common presentation was features of raised intracranial tension. There were equal numbers of Grade II and Grade III tumors. The imaging characteristics in adult and pediatric age group were similar. The tumor was large and had both solid and cystic components. Advanced imaging such as diffusion, perfusion, and spectroscopy were suggestive of high-grade tumor. Only differentiating factor between Grade II and Grade III was the presence of calcification. 1234 rule and periwinkle sign which we have described in this article may help characterize this tumor on imaging.

Conclusion: This series expands the clinical and imaging spectrum of STE and identifies characteristics that should suggest consideration of this uncommon diagnosis.

Key words: Diffusion, imaging, perfusion, spectroscopy, supratentorial ependymoma

Introduction

Supratentorial ependymoma (STE) is a rare primary glial tumor arising from ependymal cells. It has no gender predilection, and the peak manifestation is in the adult age group (mean age, 18–24 years).[1] Intraventricular, intraparenchymal forms and pure cortical forms have been described based on location.[2-4] Histologically, STE corresponds to World Health Organization (WHO) Grade II or III (Anaplastic). Though they are aggressive tumors with high recurrence rates, they are well-demarcated tumors.[5] Identifying STE is important for patient management because its malignant biologic behavior.

The largest known published cohort in the imaging literature is a case series of 21 cases.[6] Unique imaging characteristics that distinguish STE from other supratentorial tumors have not yet been identified. The aim of our present study was to review the imaging characteristics of both the intraventricular form and intraparenchymal form of STE with clinicopathological correlation.

The highlight of our study is that our case series comprises the largest cohort of 41 patients from a single center. We report some unique imaging features that when present may suggest STE.

Access this article online	
Quick Response Code:	Website: www.asianjns.org
	DOI: 10.4103/1793-5482.162702

Address for correspondence:
Prof. Vani Santosh, Department of Neuropathology, National Institute of Mental Health and Neuroscience, Bengaluru, Karnataka, India. E-mail: vani.santosh@gmail.com

Materials and Methods

This is retrospective study of computed tomography (CT) and magnetic resonance images (MRI) characteristics

of 41 cases from the neuropathology database of histopathologically proven STE on a cohort of patients treated in a single center from January 2000 to August 2012. Informed consent was obtained from Institutional Ethics Committee for this study.

Inclusion criteria were histologically proven Grade II and Grade III STE. Recurrent tumors, subependymomas (Grade I WHO classification) and ependymomas that extended into supratentorial compartment as a direct extension from infratentorium or as metastases were excluded. The slides of ependymoma were reviewed by the neuropathologist (VS) and graded as WHO Grade II or Grade III. Immunohistochemistry using the Ki-67 specific monoclonal antibody (MIB-1 from DAKO), and the MIB-1 labeling index was also assessed [Figure 1]. Preoperative CT and MRI were available in 38 cases and 8 cases, respectively. Imaging characteristics of these STEs were retrospectively reviewed. The clinical, imaging and pathological characteristics have been described in this case series. CT and MRI findings, including location, size, signal intensity, hemorrhage, and enhancement pattern, were tabulated and described separately in intraventricular and intraparenchymal forms.

Advanced MRI such as diffusion imaging, perfusion, and spectroscopic imaging findings are also available.

Results

Clinical features

A total of 41 cases of STE were encountered. Majority of cases in our case series were in the pediatric age group (<18 years, $n = 31$, 75%) with a mean age = 14.5 years and peak incidence in first decade. In the adult age group ($n = 10$, 25%), peak incidence was in 4th decade ($n = 6$, 60%) and with a male preponderance. There were four patients below the age of 3 years and one patient aged 60 years. The most common clinical presentation in the intraparenchymal form was with features of raised intracranial tension (87%). Next common were seizures (32%) and focal neurological deficit or gait disturbances (18%). On clinical examination, papilledema was most commonly noted (90%) followed by decreased visual acuity (24%), corticospinal tract involvement (32%) and facial nerve palsy (18%). Intraventricular tumor presented with features of raised intracranial tension.

Imaging features

Of the 41 cases, CT findings were available in 38 patients, and 9 cases had MRI. Three cases had only MRI with no CT imaging available for reviewing. Advanced imaging such as diffusion, susceptibility-weighted imaging (SWI), and MR spectroscopy (MRS) was available in 8 cases and perfusion was available in a single case in our series.

Based on the location (intraparenchymal or intraventricular), CT and MRI characteristics have been described separately.

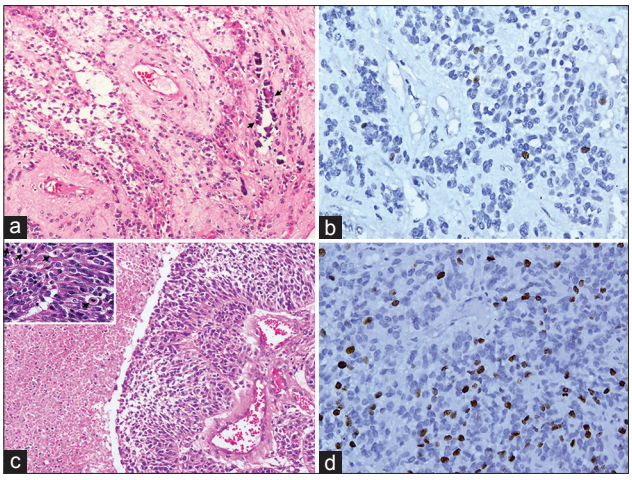

Figure 1: Microphotographs of supratentorial ependymomas: (a) H and E section showing Grade II ependymoma with calcification (arrows). (b) The tumor shows low MIB-1 labeling. (c) H and E section showing anaplastic ependymoma with increased cellularity, necrosis, and increased mitosis (inset-arrows). (d) MIB-1 labeling of this tumor is high. Original magnification ×160 for all micro photographs except inset of Figure 1c which is ×320

Intraparenchymal supratentorial ependymoma

Intraparenchymal STE were found in 37 cases and in majority, the lesion was more common in the frontal region ($n = 21$, 56%) followed by parietal region ($n = 14$, 37%). The tumor had overall predilection for left side ($n = 21$, 56%) in the frontal ($n = 7$, 18%) and parietal regions ($n = 14$, 37%). One case each with tumor in the temporal lobe and the occipital lobe was noted. The tumor was located in the periventricular zone involving the deep white matter. On CT, the intraparenchymal lesions had both solid component and a large peripheral cystic component and together their axial measurement in the entire cohort ranged between 3 and 10 cm [Figure 2a and b].

The solid component had lobulated, well-defined margins and had an axial diameter of 2–5 cm. The solid component was either isodense ($n = 24$, 64%) or hypo dense ($n = 9$, 23%) or hyperdense ($n = 5$, 13%) as compared to gray matter. Areas of large central chunky calcification were noted ($n = 30$, 78%). Postcontrast heterogeneous enhancement was noted in all the cases. Only in tumors with the solid portion >3 cm ($n = 29$, 76%) central nonenhancing area suggestive of necrosis on CT was noted. Few small foci of cystic change were also noted in the margins of the solid component which were not enhancing postcontrast.

A large well-defined peripheral cystic component homogenously isointense to the cerebrospinal fluid (CSF) was noted abutting the margins of the solid component. The cystic component was noted in 20 cases (52%), abutting either the anterior aspect ($n = 16$, 80%) or the posterior aspect ($n = 4$, 20%) of solid component. The cyst was large with axial diameter ranging between 4 and 10 cm in the 20 cases. The margins of

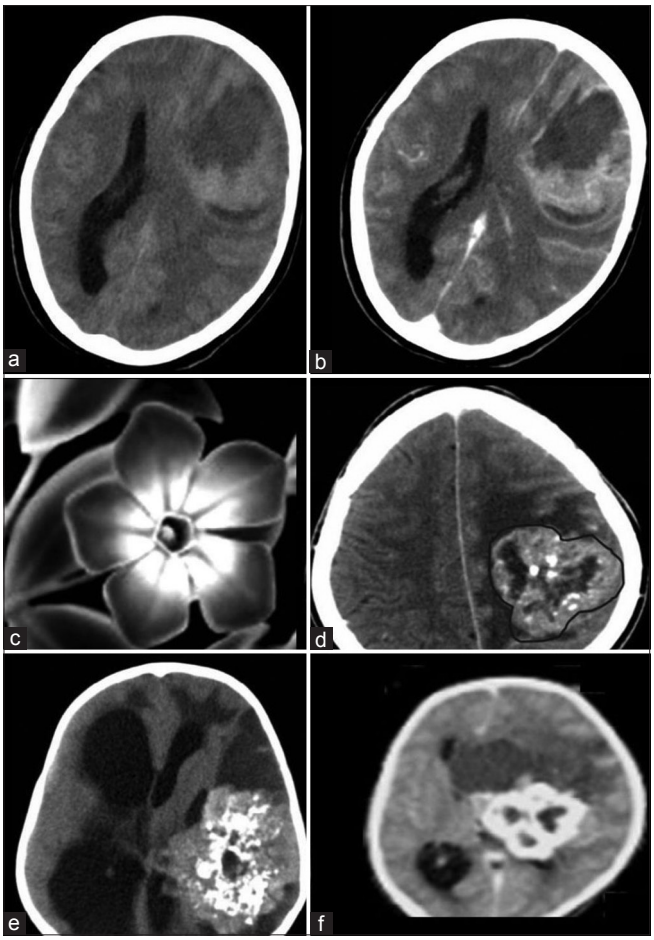

Figure 2: Supratentorial ependymoma (STE) - Intraparenchymal form: (a) Axial nonenhanced low-dose computed tomography (NECT) and (b) contrast-enhanced computed tomography (CECT). The solid component of the tumor is isodense to gray matter and shows moderate to intense enhancement on CECT. Central nonenhancing areas of necrosis are also seen. The peripheral cystic component shows enhancing margins. Periwinkle sign: (c) Black and White picture of periwinkle flower to which the tumor has been likened to Figure 2d-f. NECT axial images of the intraparenchymal form of STE show the characteristic periwinkle sign due to its lobulated margins (demarcated with a brown line in Figure 2d), central necrosis and centripetal pattern of calcification. Large peripheral cyst is also noted which has been likened to a leaf. This sign is evident with varying degree of calcification as noted in Figures 2d-f

the cyst showed contrast enhancement in all the cases. The cyst was a simple cyst on imaging with no areas of calcification or internal septa or nodule to suggest a complex cyst.

Interestingly, on CT, a unique pattern emerged and resembled the flower periwinkle. This sign was noted on axial CT sections of intraparenchymal form of STE and was produced when the large solid component had centripetal calcification of varying degree and resembled periwinkle with an associated peripheral cyst which can be likened to the leaf. This sign is well-delineated in the black and white picture of the flower and in tumor [Figure 2c-f]. In our case series, we have coined this radiologic sign as "periwinkle sign" and was noted in 6 cases (15%) on nonenhanced low-dose CT (NECT). This characteristic pattern emerges from being a simple form where margins are isodense with central calcification, to the margins becoming more hyper dense and finally becoming fully calcified on an axial NECT.

Magnetic resonance imaging was available in 8 cases. On T1-weighted images, the solid portion of the tumor was heterogeneous in intensity, varying between iso intense ($n = 6$, 71%) or hyper intense ($n = 2$, 28%) [Figure 3a]. On T2-weighted images, intensity was either hypo intense ($n = 6$, 71%) or hyper intense ($n = 2$, 28%). Areas of central T2 hyper intensity which were not inverting on fluid-attenuated inversion recovery (FLAIR) corresponded to central necrosis and areas of T2 hypo intensity blooming on gradient sequences suggested calcification. Postcontrast enhancement was moderate to intense in nature. None of the tumor showed flow voids around the lesion. Areas which were T2 hypo intense also showed restricted diffusion (71%) and may be explained as areas of high cellularity based on signal characteristics. MRS was available in all the 8 cases, and all showed choline/creatinine ratio of 4–7. Lactate peak was also noted at 1.3 ppm in four cases. Perfusion was done in one case of Grade III STE and showed increased cerebral blood volume (CBV) (approximately 5 times) and the mean time intensity curve showed a poor return to baseline [Figure 3b-f].

The large peripheral cystic component was isointense to CSF on T1 and T2 sequences and was inverting on FLAIR sequence and showed facilitated diffusion. Only a single case showed blood fluid levels in the cystic component and was confirmed on SWI, diffusion-weighted imaging (DWI) and T2 gradient echo sequences.

Intraventricular supratentorial ependymoma

The intraventricular STE constituted smaller fraction in our series ($n = 4$, 10%) and all presented in pediatric age group. They were located either in the third ventricle ($n = 3$, 75%) or in the lateral ventricle ($n = 1$, 25%).

On CT [Figure 4a], the peripheral cyst was present in one of the lesions, rest of the intraventricular STE were solid ($n = 3$, 75%). The axial dimensions ranged between 2 and 3.5 cm in the 4 cases, and the size was relatively small as compared to intraparenchymal type. The solid component was isodense to gray matter with areas of central calcification. On contrast-enhanced CT, the tumor showed moderate to intense enhancement. The peripheral cystic component was isodense to CSF and margins of the cyst showed thin walled contrast enhancement.

Magnetic resonance imaging was available in a single case [Figure 4b-d]. The tumor was heterogeneous in signal intensity and was predominantly T1 hypo intense, T2 hyper intense in relation to gray matter. Calcifications were apparent as foci of blooming on gradient images. Facilitated diffusion was

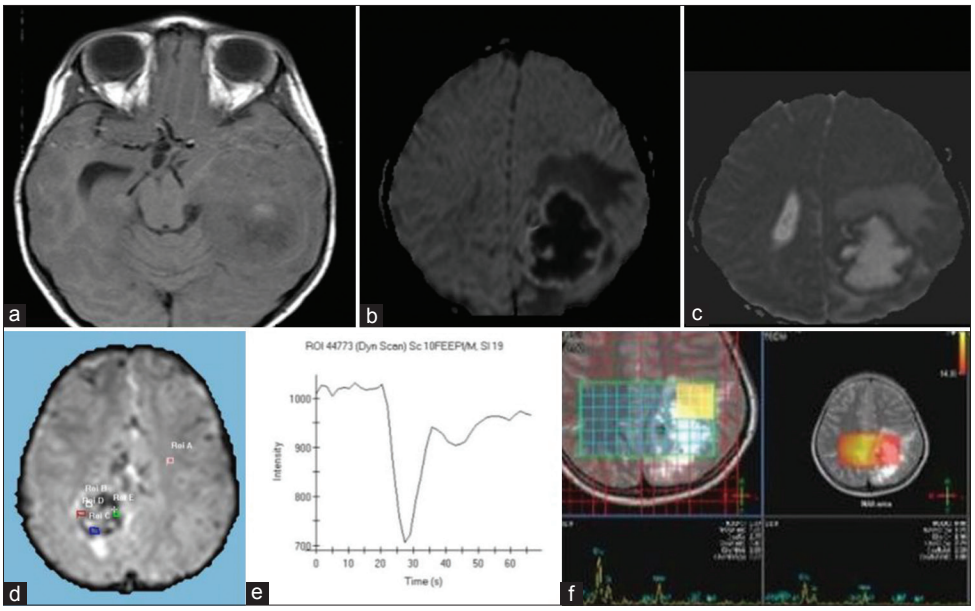

Figure 3: Supratentorial ependymoma-Intraparenchymal form: (a) Axial T1-weighted magnetic resonance image (MRI) shows central areas of hyperintensity in the tumor mass probably due to early calcification. Advanced MRI (Figure 3b-f). (b) Diffusion-weighted image sequence. (c) Apparent diffusion coefficient image. Margins of the solid component are showing high signal on diffusion-weighted imaging and low signal on apparent diffusion coefficient sequences suggestive of restricted diffusion. Rest of the tumor shows facilitated diffusion. Perilesional edema is also evident. (d) Dynamic susceptibility enhanced (DSE) Perfusion maps in another case shows increased relative cerebral blood volume in the tumor mass (approximately 5 times more) than the opposite white matter. (e) The mean intensity curve derived from the DSE perfusion image of the same case shows a poor return to baseline. (f) Multivoxel MR spectroscopy at long TE on 3T MRI in another case shows a large choline peak and decreased N-acetylaspartate peak

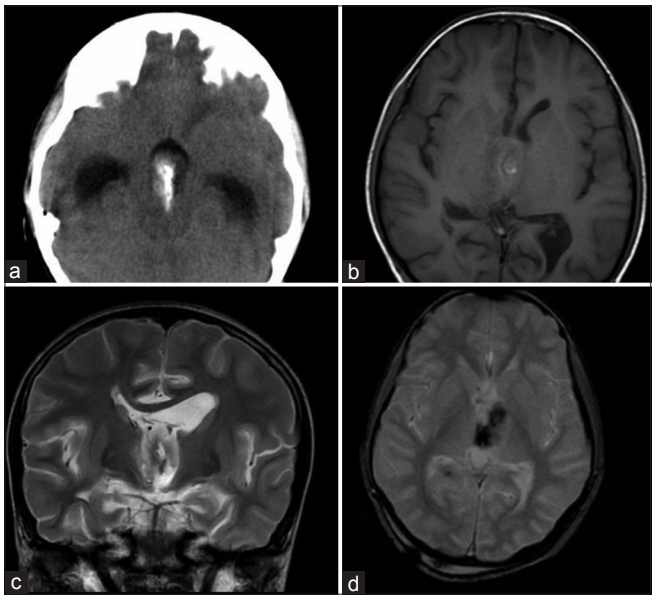

Figure 4: Supratentorial ependymona-intraventricular form: (a) Axial nonenhanced low-dose computed tomography. The tumor is isodense to gray matter and shows central calcification. Secondary hydrocephalus is also noted. (b) Axial T1-weighted (c) Coronal T2-weighted (d) Axial gradient echo magnetic resonance image of the same case shows tumor is isointense to gray matter on T1 sequence and hyperintense on T2 sequence. Central areas of calcification which are seen as T1 hyperintensity, T2 hypointensity and which are blooming on GE sequences are noted

noted on DWI. Postcontrast sequence showed intense uptake of contrast. MRS showed a raised choline to creatinine ratio of 2.

Overall the imaging characteristics were similar in both the forms of STE.

Additional imaging findings on computed tomography and magnetic resonance images

In the intraparenchymal type, hemispheric perilesional edema disproportionate to the size of tumor was noted ($n = 37$, 90%) resulting in mass effect, midline shift and hydrocephalus ($n = 13$, 34%). The lesions were purely intraparenchymal or intraventricular with no evidence of transventricular, transcortical or infratentorium extension. Hydrocephalus was present in all intraventricular STE. Though the tumor is known to be aggressive, we did not any find evidence of dissemination or metastases in both the forms of STE.

Histopathology

Incidence of Grade II and Grade III was equal. Microvascular proliferation and foci of necrosis were prominent in Grade III tumors and calcification and vascular hyalinization was prominent in Grade II tumors. The tumor type varied between classical type (80%) to papillary or clear cell type ($n = 1$). The MIB-1 LI of the tumors varied from 2% to 18%, (mean = 9.05 ± 5.2 standard deviation [SD]). The mean LI was 4.7 ± 2.6 (SD) for Grade II and 13.4 ± 2.9 (SD) for Grade III, respectively.

Imaging and age correlation

Imaging characteristics of solid and cystic component were similar in all age groups, and there was no definite differentiating factor.

Detailed findings noted in one case each involving extremes of age in a 2-year-old child and 60-year-old female are described. In the child with Grade III tumor, we found the cystic component to have a blood fluid level on MRI, and solid component showed restricted diffusion and increased relative CBV (rCBV) on perfusion maps with high choline/creatinine ratio and reduced N-acetylaspartate (NAA) on MRS which was later confirmed to be Grade III STE. In 60-year-old female, the tumor was isodense with multiple small and scattered cystic foci with no areas of calcification or necrosis in the solid component, and a large peripherally placed cyst. Disproportionate perilesional edema, hydrocephalus, and postcontrast enhancement were noted. The clinical and CT findings were very similar to metastases except for a large cystic component which was the only clue for an STE to be the diagnosis in this case.

Imaging and histopathology correlation

Calcification was more common in Grade II than in Grade III and was the only imaging finding differentiating the two. Large peripheral cyst was noted in both Grade II ($n = 9$) and III ($n = 11$) and was not a differentiating factor. No other characteristic pattern was available either on CT, basic MR or advanced MRI sequences such as DWI, Perfusion or spectroscopy.

Discussion

Supratentorial ependymoma accounts for 30–50% of all intracranial ependymomas.[3,7] The peak manifestation has been described in adult age group with mean age of 18–24 years[1,8] with nearly 50% in second and third decade, however, in our case series, the mean age of presentation was 14.5 years and was more common in the first decade. The clinical presentation depends on the tumor location intraventricular form presents with features of raised ICT whereas the intraparenchymal form presents with focal neurologic deficits, headache, and seizures.[1] The incidence of Grade II and Grade III tumor was equal with the classical variant noted in the majority of cases (80%) and is in concordance with literature.[5] The MIB-1 L1 was 4.25 and 13.4 in Grade II and Grade III, respectively, in STE. Karamitopoulou *et al*.[9] have described MIB-1 L1 index in ependymoma in general and was 2.6 and 6.89 in Grade II and Grade III ependymoma, respectively. The higher index in our study may be due to the fact that labeling index was described only for STE, and this entity has high recurrence rates.

Intraparenchymal form arises purely from the white matter and is homogenous granular, solid mass with associated cystic element, necrotic foci or hemorrhage. They have definite ependymal morphology on histopathology, and it has been hypothesized that they originate from the embryonic ependymal remnants in the brain parenchyma This form of STE has a predilection for frontal, temporal or parietal lobe.[10] The intraventricular form of STE occupies and expands the CSF cavity. Occasionally, they can invade the brain parenchyma.

On imaging among the two forms of STE, intraparenchymal formed the majority as compared to the intraventricular form though other studies have described equal incidence ratio of both the forms.[3] Intraventricular form of STE was not noted in the adult age group although the pure cortical form has been described in the literature,[10] this form was not noted in our series.

Supratentorial ependymomas more often contain a separate solid and cystic component as compared to infratentorial ependymomas.[11] In the intraparenchymal form, the parietal lobe and frontal lobe was most common site.[12] STE were large tumors, and it has been hypothesized that this is due to its supratentorial location.[6]

On CT, similar to as described in other studies,[2,6,11-13] these tumors were isodense, hyper or hypo dense to the cerebral cortex. Intratumoral calcification is present in one-third of the cases.[6] Heterogenous moderate to intense enhancement of the solid component and enhancement of cyst margins was noted in our series. Few foci of low-density necrotic areas were noted in large tumors. Associated secondary findings include hydrocephalus and peritumoral edema (50%). Areas of hemorrhage in the solid component have been described in other studies[6] though on correlation of CT with T1 and T2 gradient sequence of MRI we did not find any areas of hemorrhage in our series. The cystic component was a simple cyst in our series. However, complex peripheral cyst has been described.[2] The periwinkle sign on axial NECT of the intraparenchymal form of STE has been described for the first time in our series.

On MRI, the intraparenchymal form of STE is described as showing prolonged T1 and T2 relaxation.[2] On T1 image, they are either hypo intense or isointense and on T2 images, they are isointense to hyper intense.[2] In two cases, foci of T1 hyper intensity were noted within probably due to early calcification as no corresponding areas of bleed were noted on the CT, gradient echo or SWI sequences although studies quote that these foci could represent methemoglobin, hemosiderin, necrosis, or calcification.[14] The cystic component was following CSF intensity in all sequences except in one case where blood fluid level was noted.

Advanced MRI techniques such as diffusion perfusion and spectroscopic imaging reflect findings of its malignant behavior on histopathology. On advanced imaging such as diffusion sequence areas of high cellularity showing T2 hypointensity and restricted diffusion were noted and helped differentiate from necrotic foci which show facilitated diffusion. The cystic portion of tumor showed facilitated diffusion in all cases. MRS with short TE has described in a series as showing increased glutamine and glutamate.[15] In our series, spectroscopy at long TE = 144 showed reduced NAA, choline/creatinine ratio of 4–7 and a lactate peak at 1.3 ppm which is suggestive of

anaerobic metabolism. Though MRS does not present with any characteristic marker in STE, it may aid to differentiate Grade II from Grade III and in cases of recurrence.[16,17] Perfusion MRI using T2* weighted dynamic susceptibility has been described in STE and demonstrated markedly elevated CBV with a poor return to baseline. The rCBV was increased approximately 5 times more in our case with Grade III tumor. This has been attributable to fenestrated blood vessels and an incomplete blood–brain barrier.[18]

In our series, the intraventricular form was more common in the third ventricle than in lateral ventricle. On comparing characteristics of the intraparenchymal and intraventricular form incidence of intraparenchymal form was much higher with intraventricular form exclusively noted only in the pediatric age group. On imaging, the size of the intraparenchymal tumor was larger. The signal characteristics of the solid and cystic component in both these forms were similar with areas of central calcification noted in both. The incidence of a large peripheral cyst and central necrosis was more common in the intraparenchymal form than in intraventricular form and may be related to its larger size. On correlating CT findings with histopathology, calcification on CT was more common in low-Grade II (60%) than high-Grade III (27%). No other characteristic finding was noted to differentiate Grade II from III.[2]

To summarize the characteristics of STE in our series, we have formulated a simple "1234 rule" 1 stands for a single large tumor common in the first decade, 2P for Perilesional edema and Periwinkle sign, 3L for Large Lobulated Lobar mass and 4C for Central Chunky Calcification and large peripheral Cyst on imaging and this may aid in differentiating intraparenchymal STE from other supratentorial tumors.

Conclusion

Our study is the largest single institution study from a cohort of patients from NIMHANS reviewing in detail the CT, MR and advanced MRI findings with clinicopathological correlation. The other highlight of this study is the description of a new sign, the "periwinkle sign" and a "1234 rule."

References

1. Koeller KK, Sandberg GD, Armed Forces Institute of Pathology. From the archives of the AFIP. Cerebral intraventricular neoplasms: Radiologic-pathologic correlation. Radiographics 2002;22:1473-505.
2. Furie DM, Provenzale JM. Supratentorial ependymomas and subependymomas: CT and MR appearance. J Comput Assist Tomogr 1995;19:518-26.
3. Goodkin R, Zaias B, Michelsen WJ. Arteriovenous malformation and glioma: Coexistent or sequential? Case report. J Neurosurg 1990;72:798-805.
4. Ono S, Ichikawa T, Ono Y, Date I. Large supratentorial ectopic ependymoma with massive calcification and cyst formation – Case report. Neurol Med Chir (Tokyo) 2004;44:424-8.
5. Rosenblum MK. Ependymal tumors: A review of their diagnostic surgical pathology. Pediatr Neurosurg 1998;28:160-5.
6. Armington WG, Osborn AG, Cubberley DA, Harnsberger HR, Boyer R, Naidich TP, *et al.* Supratentorial ependymoma: CT appearance. Radiology 1985;157:367-72.
7. Schiffer D, Chiò A, Giordana MT, Migheli A, Palma L, Pollo B, *et al.* Histologic prognostic factors in ependymoma. Childs Nerv Syst 1991;7:177-82.
8. Shuangshoti S, Rushing EJ, Mena H, Olsen C, Sandberg GD. Supratentorial extraventricular ependymal neoplasms: A clinicopathologic study of 32 patients. Cancer 2005;103:2598-605.
9. Karamitopoulou E, Perentes E, Diamantis I, Maraziotis T. Ki-67 immunoreactivity in human central nervous system tumors: A study with MIB 1 monoclonal antibody on archival material. Acta Neuropathol 1994;87:47-54.
10. Hamano E, Tsutsumi S, Nonaka Y, Abe Y, Yasumoto Y, Saeki H, *et al.* Huge supratentorial extraventricular anaplastic ependymoma presenting with massive calcification – Case report. Neurol Med Chir (Tokyo) 2010;50:150-3.
11. Morrison G, Sobel DF, Kelley WM, Norman D. Intraventricular mass lesions. Radiology 1984;153:435-42.
12. Lehman NL, Jorden MA, Huhn SL, Barnes PD, Nelson GB, Fisher PG, *et al.* Cortical ependymoma. A case report and review. Pediatr Neurosurg 2003;39:50-4.
13. Osborn AG, Daines JH, Wing SD. The evaluation of ependymal and subependymal lesions by cranial computed tomography. Radiology 1978;127:397-401.
14. Spoto GP, Press GA, Hesselink JR, Solomon M. Intracranial ependymoma and subependymoma: MR manifestations. AJR Am J Roentgenol 1990;154:837-45.
15. Panigrahy A, Krieger MD, Gonzalez-Gomez I, Liu X, McComb JG, Finlay JL, *et al.* Quantitative short echo time 1H-MR spectroscopy of untreated pediatric brain tumors: Preoperative diagnosis and characterization. AJNR Am J Neuroradiol 2006;27:560-72.
16. Barkovich AJ. Pediatric Neuroimaging. 4th ed. Philadelphia: Lippincott Williams and Wilkins; 2005.
17. Yuh EL, Barkovich AJ, Gupta N. Imaging of ependymomas: MRI and CT. Childs Nerv Syst 2009;25:1203-13.
18. Uematsu Y, Hirano A, Llena JF. Electron microscopic observations of blood vessels in ependymoma. No Shinkei Geka 1988;16:1235-42.

How to cite this article: Mangalore S, Aryan S, Prasad C, Santosh V. Imaging characteristics of supratentorial ependymomas: Study on a large single institutional cohort with histopathological correlation. Asian J Neurosurg 2015;10:276-81.

Source of Support: Nil, **Conflict of Interest:** None declared.